Journal of Geodynamics 51 (2011) 327–338

Contents lists available at ScienceDirect

Journal of Geodynamics

journal homepage: http://www.elsevier.com/locate/jog

# Rotation history of Chios Island, Greece since the Middle Miocene

D. Kondopoulou [a], S. Sen [b], E. Aidona [a,*], D.J.J. van Hinsbergen [c], G. Koufos [d]

[a] Department of Geophysics, School of Geology, Aristotle University of Thessaloniki, 54124 Thessaloniki, Greece
[b] Department de la Terre, Musuem d'Histoire Naturelle, 8, rue Buffon, 75005 Paris, France
[c] Physics of Geological Processes, University of Oslo, Sem Sælands vei 24, 0316 Oslo, Norway
[d] Department of Geology, School of Geology, Aristotle University of Thessaloniki, 54124 Thessaloniki, Greece

ARTICLE INFO

*Article history:*
Received 2 November 2009
Received in revised form 21 July 2010
Accepted 21 July 2010
Available online 30 July 2010

*Keywords:*
Aegean
Paleomagnetism
Vertical axis rotation
Chios

ABSTRACT

Superimposed on a regional pattern of oroclinal bending in the Aegean and west Anatolian regions, the coastal region of western Anatolia, shows a complex and chaotic pattern of coexisting clockwise and counterclockwise rotations. Here, we report new palaeomagnetic data from the eastern Aegean island of Chios, to test whether this fits the regional palaeomagnetic pattern associated with the Aegean orocline, or should be included in the narrow zone of chaotic palaeomagnetic directions. Therefore, a combined palaeomagnetic study of Miocene sediments and volcanic rocks has been carried out. Thermal and AF demagnetization of a 130-m thick Middle Miocene succession from the Michalos claypit allowed a stable component of both polarities to be isolated while rock magnetic experiments showed that the main magnetic carrier is magnetite. When compared with the Eurasian reference, the mean declination of $348 \pm 5.1^\circ$ implies $15^\circ$ of counterclockwise rotation since Middle Miocene times. The obtained shallow inclination of $38 \pm 6.7^\circ$ was corrected to $61.8 \pm 3.9^\circ$, by applying the elongation/inclination correction method for inclination shallowing. This result is similar to the expected inclination of $58^\circ$ for the latitude of Chios. The palaeomagnetic analysis (demagnetization treatment and corresponding rock magnetic measurements) of the volcanic rocks identify a stable, predominantly normal, ChRM with poorly constrained mean declination of about $290 \pm 19.8^\circ$ based on five successfully resolved components. The significantly different palaeomagnetic results obtained from an island as small as Chios (and a very short distance), and the relatively large rotation amounts do not fit the regional palaeomagnetic direction of Lesbos and basins in northwestern Turkey which show little or no significant rotation. We thus prefer to include Chios in the coastal zone of chaotic rotations, which may represent a previously inferred tectonic transfer zone that accommodates lateral differences in extensional strain within the Aegean back-arc.


## 1. Introduction

The southern Aegean and west Anatolian regions display a curved orogenic belt that formed upon subduction of oceanic and continental crust during northward subduction since the Cretaceous (Şengör and Yilmaz, 1981; Jacobshagen, 1986; van Hinsbergen et al., 2005a; Jolivet and Brun, 2010). Since subducting lithosphere attached to the African Plate started to roll back in late Eocene or Oligocene times, major crustal thinning and exhumation of metamorphic rocks along extensional detachments has occurred in the back-arc region of the Aegean (Gautier and Brun, 1994; Jolivet et al., 1994; Bozkurt and Oberhänsli, 2001; Jolivet, 2001; Ring et al., 2001; Brun and Sokoutis, 2007; Forster and Lister, 2009; Ring et al., 2010).

Since Middle Miocene times, the external parts of the Aegean and west Anatolian regions have been affected by major, regional and local vertical axis rotations that shaped the Aegean orocline (Kissel and Laj, 1988; Duermeijer et al., 2000; Kondopoulou, 2000; Aidona et al., 2008; van Hinsbergen et al., 2005b, 2008). The western Aegean region has experienced a coherent, ~40° clockwise rotation with respect to the Moesian platform since ~15 Ma (Kissel and Laj, 1988; van Hinsbergen et al., 2005b, 2008), during which internal south-western Turkey has experienced a simultaneous ~20° counterclockwise rotation (Kissel and Poisson, 1987; Morris and Robertson, 1993; van Hinsbergen et al., 2010a,b). The clockwise rotation of the Western Aegean extends further to the NE via progressive decrease in CW rotation to about ~20° (Westphal et al., 1991; Atzemoglou et al., 1994; Zananiri et al., 2002). In the north, the orocline is limited by the non-rotating Moesian platform (van Hinsbergen et al., 2008), which is generally considered to be part of the Eurasian continent (e.g. Ricou et al., 1998; Schmid et al., 1998). In the vicinity of the North Anatolian Fault Zone, Northwestern Turkey displays a pattern of variable rotations (Piper et al., 2009 and references therein), whereas to the south, outside of the influence of NAFZ, the Eastern Aegean Island of Lesbos and lower Miocene basins and volcanic centers in western Turkey do not appear to

* Corresponding author. Tel.: +30 2310998594; fax: +30 2310998528.
*E-mail address:* aidona@geo.auth.gr (E. Aidona).

0264-3707/$ – see front matter © 2010 Elsevier Ltd. All rights reserved.
doi:10.1016/j.jog.2010.07.001

have experienced significant vertical axis rotations (Kissel et al., 1989; Beck et al., 2001; van Hinsbergen et al., 2010a). Northwestern Turkey is not a part of Aegean oroclinal bending and is separated from the rotating domains by extensional ones in the Aegean back-arc (van Hinsbergen et al., 2010a). Vertical axis rotations of the external domains of the Aegean and west Anatolian region were in part accommodated by Neogene extension and exhumation of metamorphic core complexes in the Aegean back-arc and in the west Anatolian Menderes Massif (Brun and Sokoutis, 2007; van Hinsbergen et al., 2010a).

Apart from these regionally coherent rotations, many regions in the area are affected by large, local rotations usually interpreted to reflect block rotations within a strike-slip regime. Careful regional analyses of these zones of local strong rotations may help to outline important transform boundaries. For instance, in the southern Aegean region, consistently counterclockwise rotations with strongly varying amounts are related to the South Aegean strike-slip system (Duermeijer et al., 1998; van Hinsbergen et al., 2007), which has been interpreted to reflect block rotations close to a slab transform edge propagator fault (Govers and Wortel, 2005). The North Anatolian Fault Zone and its equivalents in northern Greece form another clear example of chaotic, strike-slip related rotations (Westphal and Kondopoulou, 1993; Kaymakci et al., 2007; Kondopoulou et al., 2007; Piper et al., 2009).

The eastern Aegean islands and the coastal zone of western Anatolia seem to be characterized by strongly varying vertical axis rotations. Whereas the majority of Neogene sedimentary basins in western Turkey seem not to display vertical axis rotations (van Hinsbergen et al., 2010a), the coastal volcanic regions of Dikili, Yuntdağ and Foca as well as the Karaburun peninsula of western Turkey show a chaotic pattern of palaeomagnetic directions (Kondopoulou and Lauer, 1984; Kissel et al., 1986a,b, 1989; Sen and Valet, 1986; Kissel and Laj, 1988; Orbay et al., 2000; van Hinsbergen et al., 2010a) (Fig. 1). It has been proposed that these rotations may reflect motion along a transform fault accommodating a larger amount of back-arc extension on the western (Aegean) side than on the eastern (Anatolian) side (Ring et al., 1999a; Özkaymak and Sözbilir, 2008; Uzel and Sözbilir, 2008; van Hinsbergen et al., 2010a).

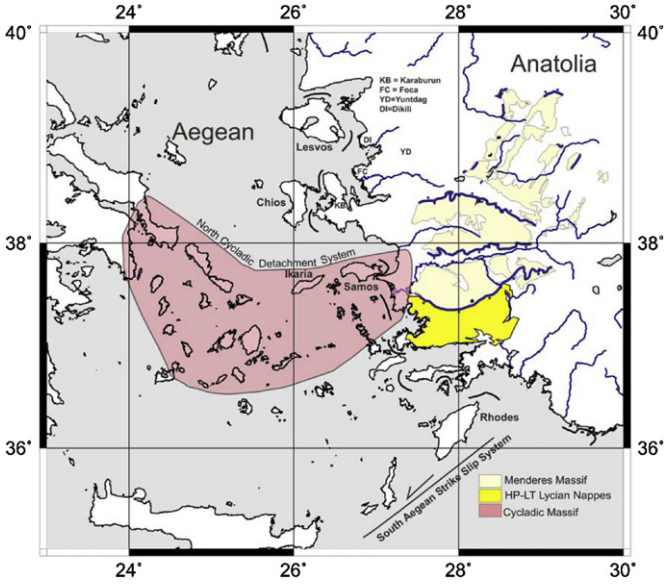


**Fig. 1.** Schematic map of eastern Aegean and western Turkey, showing the distribution of the main crystalline Cyclades and Menderes massifs, and the high-pressure, low temperature (HP–LT) Lycian Nappes (see Jolivet et al., 2010; van Hinsbergen et al., 2010b and references therein for details on these massifs).

In this paper, we study the post-Middle Miocene vertical axis rotation history of the island of Chios, located in the hanging wall of the major extensional detachments of the Cyclades, which exhumed metamorphosed rocks on the islands of Samos and Ikaria to the south of Chios (Ring et al., 1999b; Kumerics et al., 2005). Chios, however, lies to the west of the Menderes metamorphic core complex of western Turkey, where exhumed metamorphosed rocks continue much further to the north than in Greece (Fig. 1) (Bozkurt and Oberhänsli, 2001; Işik and Tekeli, 2001; Ring et al., 2003; Işik et al., 2004). We will discuss the results within the light of the regional rotation picture of the Aegean and west Anatolian region.

## 2. Geology of Chios Island

Chios exposes a Palaeozoic clastic succession and Mesozoic recrystallized limestones unconformably overlain by Cenozoic formations (Fig. 2; Kilias, 1982). In the southeast, terrestrial Neogene deposits have been recognised as fossiliferous by vertebrate paleontologists since 1940 when Paraskevaidis (1940) described the Middle Miocene mammal fauna from the Michalos clay pit.

In the Michalos clay pit, as well as in the surrounding area, the Neogene deposits are well-exposed, and the changing sedimentary environment can be studied in continuous outcrops over hundreds of meters. The Michalos section, with several mammal bearing horizons, is probably one of the most complete sections in Europe to display an Early-Middle Miocene marine to terrestrial transition. In this section, three horizons were recorded with abundant remains of small and large mammals. Their faunas date the fossiliferous horizons to the earliest part of the Middle Miocene, known as the MN5 zone (Koufos et al., 1995). The presence of a rich mammalian fauna and a continuous stratigraphic succession has stimulated investigation of magnetostratigraphy. A total of 99 levels from a 130-m thick section have been sampled for palaeomagnetic study. Preliminary magnetostratigraphic results were published by Kondopoulou et al. (1993a) and Sen et al. (2006) while detailed magnetostratigraphic results and palaeontological correlations will be presented later (Sen et al., under prep.). Here we focus on the tectonic implications of the palaeomagnetic findings, for which a dating of Middle Miocene MN5 will suffice.

In addition to the Neogene sediments, the island of Chios contains a series of small volcanic centers in the northwest and southeast, which developed during the same time interval as the deposition of the Michalos section (Besenecker and Pichler, 1974). The source magmas have several features comparable to ocean island basalts and resemble subduction – related rocks (Pe-Piper and Piper, 1989). K/Ar radiometric dating on whole rock samples indicates volcanic activity between 17 and 14 Ma (Bellon et al., 1979).

The broader Chios – Karaburun region displays complex tectonics. Seismic reflection data show onshore and offshore deformation in Western Turkey dominated by crustal extension, and strike-slip (Ocakoğlu et al., 2005; Uzel et al., 2010). Approximately E–W trending grabens and basin-bounding active normal faults are the most prominent young tectonic features of this part of Western Turkey.

Active tectonism in the study area was first described by Besenecker (1973) and Bellon et al. (1979). A detailed study with microtectonic measurements and fault observations on SE Chios identify sinistral movement on a system of parallel faults directed generally NNW–SSE, within a small distance (few kilometers) from the region of the sampling area of this study (Kondopoulou et al., 1993b). This system of faults belongs to the basement and is related to dextral transtensional or extensional movements and has been reactivated during the Quaternary with a sinistral normal movement. Neogene deposits are also faulted, indicating an

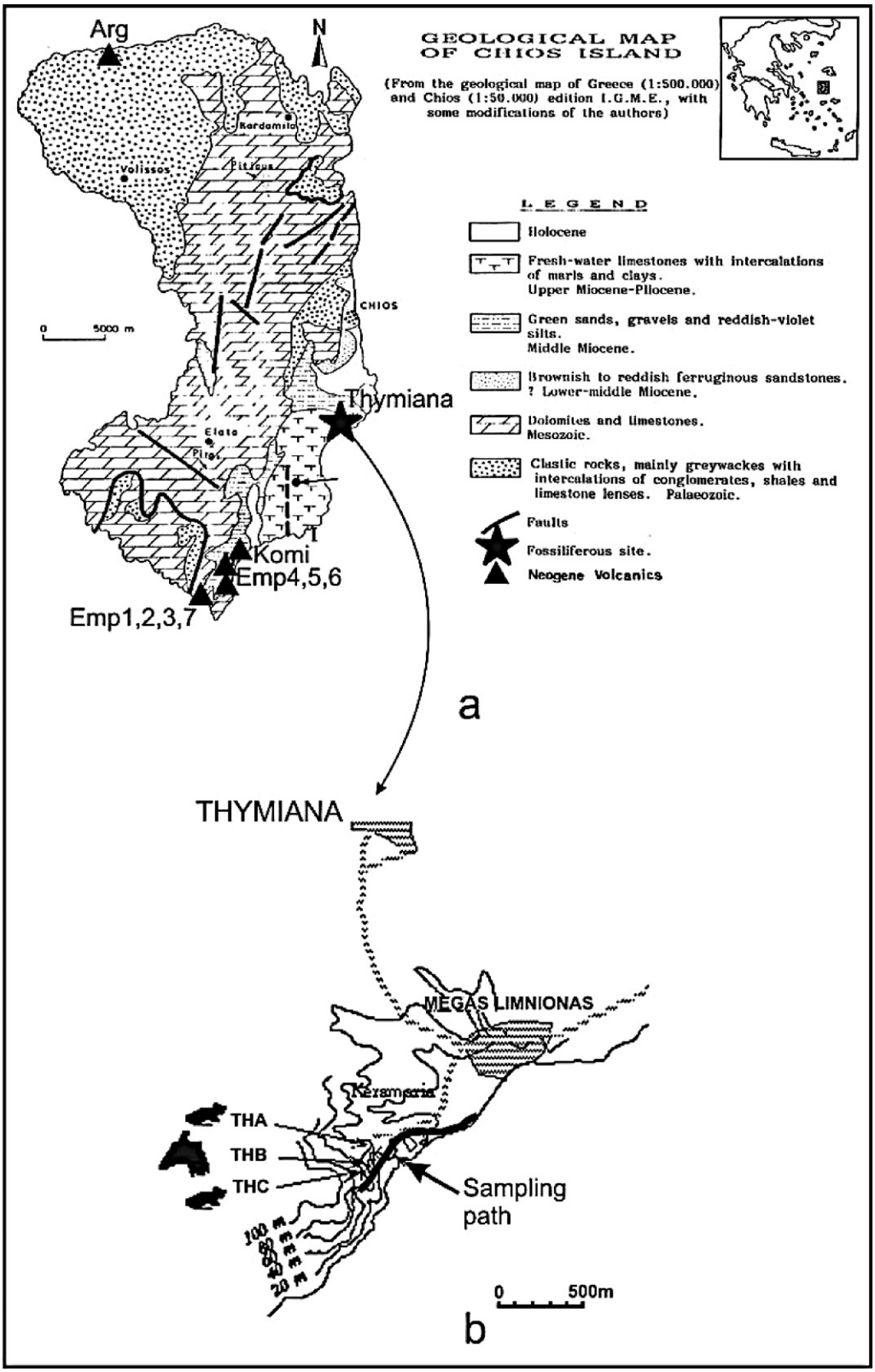


**Fig. 2.** (a) Geological map of Chios Island. Asterisk shows the location of the sampled sedimentary section, and triangles represent the sampling sites of lavas. (b) Detailed map of the sampling path for the magnetostratigraphic study. THA, THB and THC are the mammal bearing horizons.

active tectonic regime in the area since their deposition. Additionally, recent study of the microseismicity of the area (Karakostas et al., 2010) shows fault plane solutions exhibiting a complex pattern of dextral and sinistral strike-slip motions, and transtensional motions as well as extension in two directions.

## 3. Sampling and measurements

For the magnetostratigraphic study, the continuous Michalos section with a thickness of 130 m was sampled. The section covers the upper part of the Zyfia formation (10 m) and almost the entire

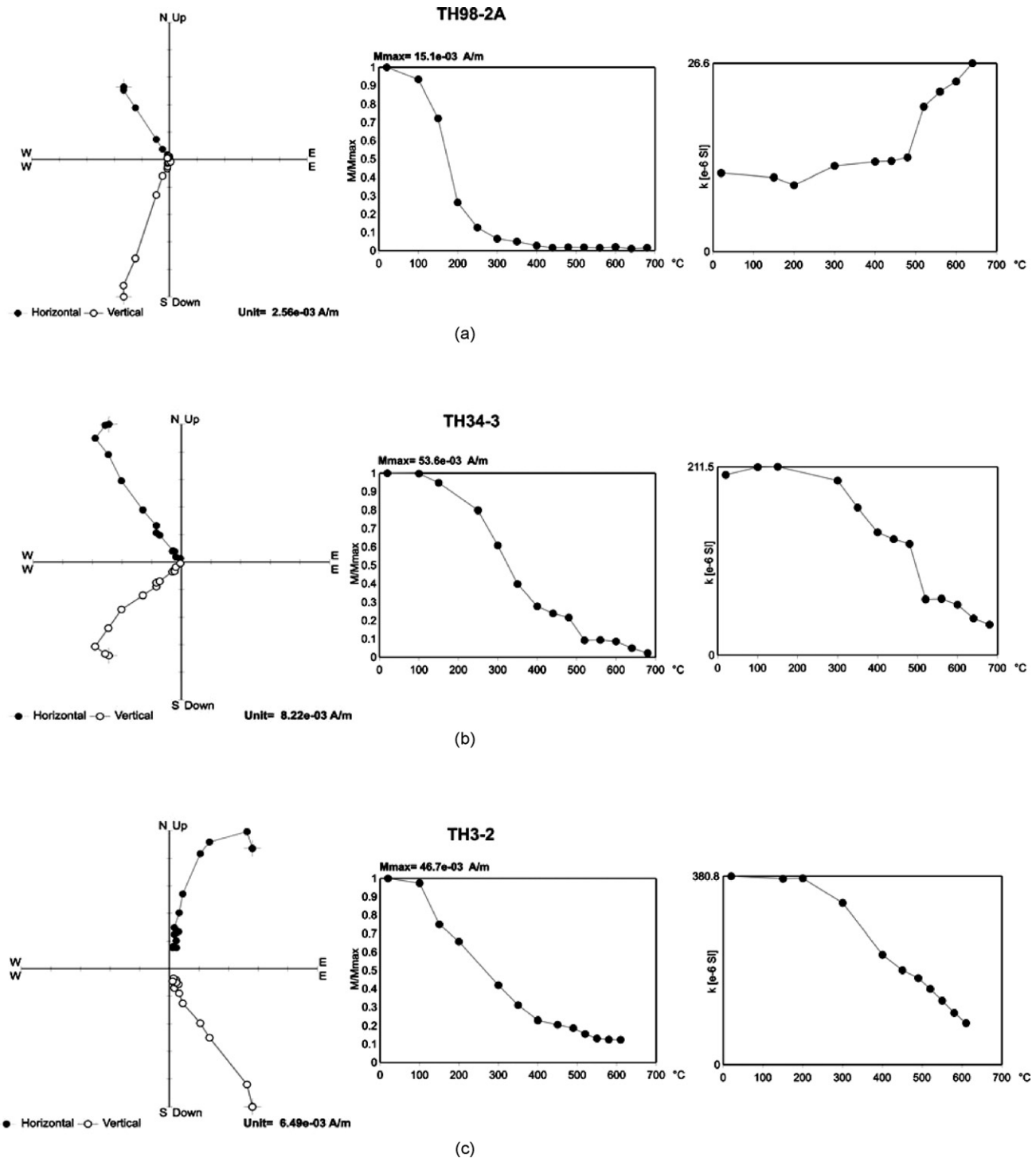


**Fig. 3.** Typical Zijderveld diagrams, intensity decay curves and variation of the magnetic susceptibility during the demagnetization process for representative sediment samples. (a) Demagnetization behavior of selected sample from the lower half of the section. The intensity decay curve shows a sharp drop at about 200 °C indicating the presence of a soft component of magnetization.

Keramaria Formation (120 m). The base of the section is limited by the lack of outcrops while its top is limited by an E–W trending normal fault. The three mammalian localities identified as THA, THB and THC, Koufos et al., 1995, are situated within the sampling section, at 72, 83 and 89 m, respectively above the base. Some of the fossiliferous localities mentioned by Rothausen (1977) and Tobien (1977) are also within this section, and are all stratigraphically bracketed between THA and THC.

Ninety-nine (99) levels with a minimum of three drilled cores per level were collected throughout this section. Samples were mainly taken from fine grained sediments such as clays, limestones and siltstones. Sampling spanned all main lithologies, with an average interval of 1.25 m. The middle part of the section was sampled more intensively than the other parts. The largest sampling intervals (maximum gap of 6.5 m near the top of the sampled section) are mainly due to the presence of levels with coarse or unconsolidated sediments. We sampled all lithologies suitable for magnetostratigraphy. Along the section, the beds dip gently towards the west, with an average strike and dip of 160°/6 ± 2° W.

The largest volcanic outcrops occur in the southeastern part of the Island where the main sampling took place. Thus in the area of Emporios (~16 Ma: Bellon et al., 1979) the andesite columnar outcrops of Komi have been sampled as well as the rhyolites in Mavra Votsala and Vroulidia. Additionally, samples have been taken from the rhyolite outcrop in the north part of the island between Agii Pantes and Kambi (Fig. 2). A total of 80 core samples were collected from these volcanic rocks and cut into standard (2.2 cm × 2.5 cm) cylindrical specimens.

Measurements of the NRM have been performed in a non-magnetic room using either spinner or three-axis cryogenic magnetometers, according to the nature of the samples. The majority of the palaeomagnetic measurements on the sediments were performed in the Laboratoire de Paléomagnétisme of the IPG in Paris, while the palaeomagnetic study of lavas took place in the Palaeomagnetic Laboratories of the University of Thessaloniki and Ecole Normale Supérieure in Paris.

At least one specimen per core has been stepwise demagnetized, in most cases thermally, from room temperature up to 600 °C or more in some cases. Alternating field demagnetization has also been used, especially for the lavas. In order to identify the magnetic carriers, in sediments and lavas, IRM acquisition curves have been obtained on samples from different levels and lithologies. Furthermore, thermal demagnetization (up to 680 °C) of the IRM has been performed in selected samples. Finally, the variation of magnetic susceptibility with temperature of pilot samples both from sediments and lavas has been examined using the MS2B Susceptibility Temperature Bartington Bridge.

## 4. Results

A total of 230 specimens from the sediments and 65 from the lavas have been demagnetized and the results obtained can be summarized as follows.

### 4.1. Sediments

The intensity of the natural remanent magnetization (NRM) is highly variable throughout the section, ranging from 0.5 to 147 mA/m. Thermal demagnetization of pilot samples identified large secondary magnetizations which could only be removed at temperatures above 250 °C. For this reason, more than 95% of the samples have been demagnetized by progressive thermal cleaning; the alternating field has been applied on some test samples, without reliable results. In some cases, when the stepwise thermal demagnetization produced a sudden increase of the susceptibility between the 400° and 500° steps (see below), both thermal and alternating field demagnetization was applied but this dual approach proved unable to completely isolate the primary component of magnetization.

All samples have been demagnetized stepwise, from room temperature up to 600 °C or more in some cases (Fig. 3b and c). The steps were performed every 50 °C in low temperatures, and every 40 °C or even 30 °C in high temperatures. The demagnetization process shows that in 53 out of 99 sites, more than half of the NRM intensity is removed at 200 °C. These sites are mainly located at the lower half of the section. After this step, the decrease of intensity of magnetization is much smoother up to 550–600 °C (Fig. 3a).

The mean direction of the characteristic remanent magnetization (ChRM) could easily be calculated in most samples using Kirschvink (1980) analysis. About 1/3 of the samples present random directions at temperatures over 400 °C, mostly connected with a sudden susceptibility increase at 450–500 °C. In these samples, the demagnetized vector gradually changes between room temperature and about 450 °C towards a stable direction, which we interpret as the direction of the ChRM.

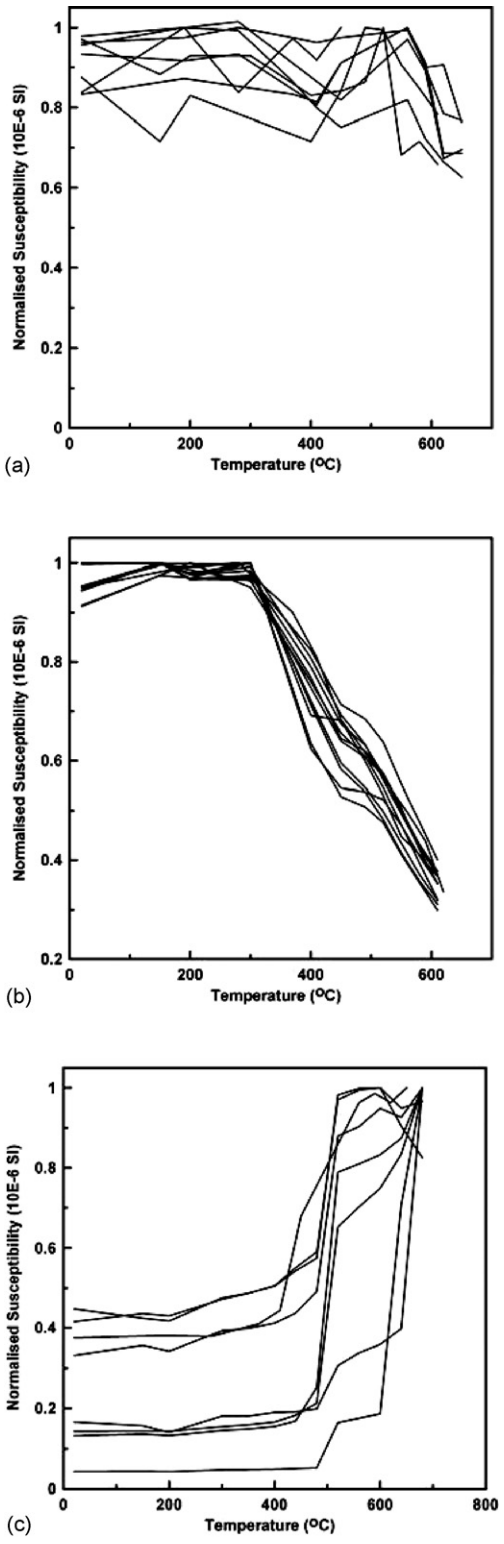


**Fig. 4.** Variation of magnetic susceptibility during thermal demagnetization. (a) The magnetic susceptibility remains stable during the experiment, only in a few cases. (b) The magnetic susceptibility decreases after 300–400 °C up to 600 °C and (c) in some cases displays a sudden increase from 450 to 500 °C.

The magnetic susceptibility was monitored with a Kappabridge after each step of heating. The susceptibility remained stable in only a few cases (Fig. 4a). In most cases it decreased progressively from 300–400 °C up to 600 °C or displayed a sudden increase from 450 to 500 °C (Fig. 4b and c, respectively). The decreasing susceptibil-

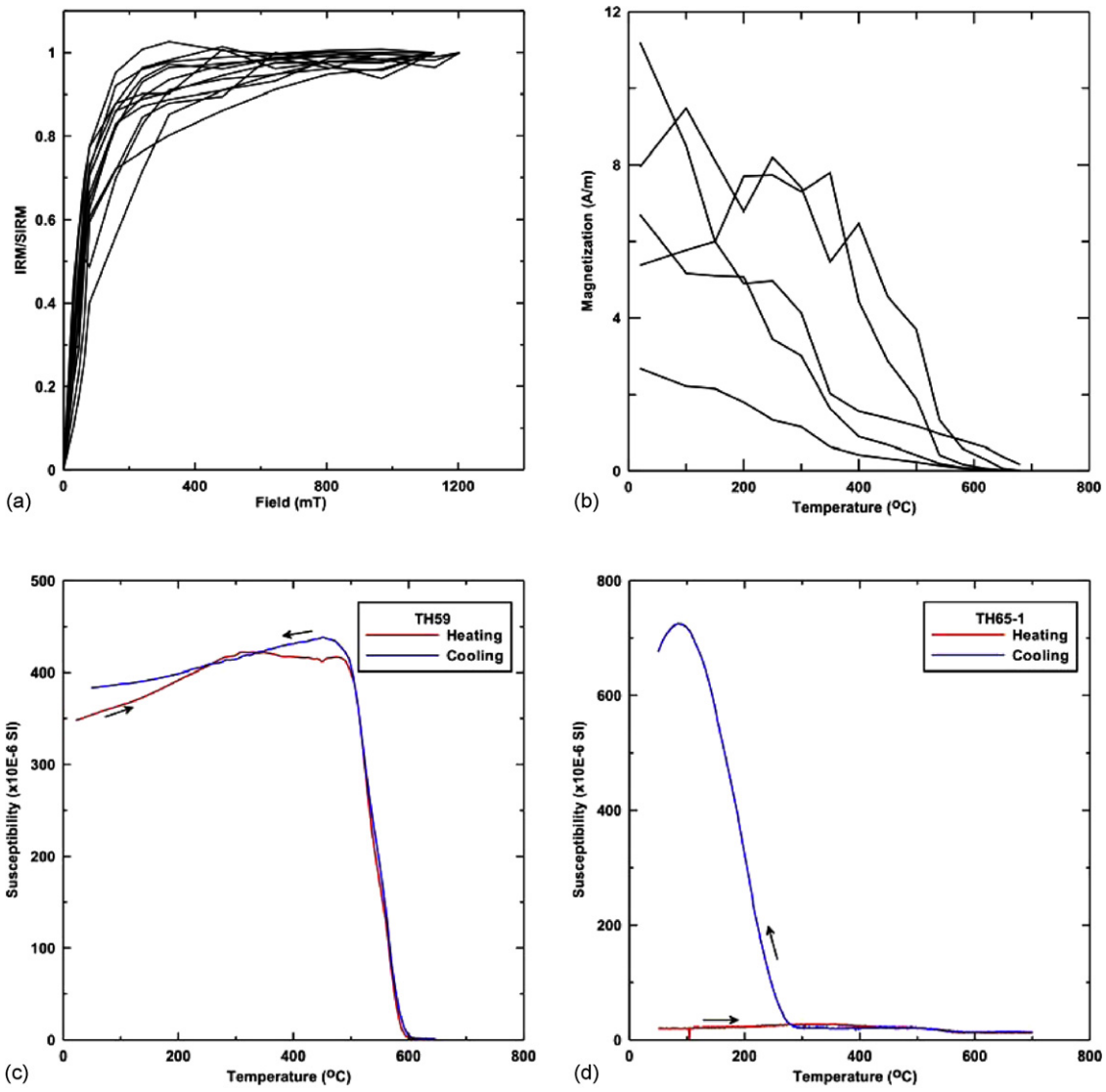


**Fig. 5.** (a) IRM curves for selected samples showing the dominance of magnetite. Only in few cases, the saturation is not complete indicating the presence of a high coercivity magnetic mineral. (b) Thermal demagnetization of the IRM (see text for details). (c) Thermomagnetic curve confirming the dominance of magnetite and (d) non-reversible thermomagnetic curve, indicating mineralogical changes of the magnetic carriers.

ity is characteristic of samples from the upper and middle parts of the section, while the increasing susceptibility is only observed in sediments from the lower part. The decrease in susceptibility generally corresponds to the removal of the secondary overprint of magnetization. The observed increase of susceptibility of the lower part usually coincides with an intensity increase. Both susceptibility and intensity changes indicated mineralogical changes of the magnetic carriers as is shown by the non-reversibility in the heating and cooling cycles of the corresponding thermomagnetic curves (Fig. 5d).

The IRM curves are consistent with magnetite as the dominant carrier (Dunlop and Özdemir, 1997), although in some cases saturation is not complete at 0.3 T, indicating the presence of a high coercivity magnetic mineral (Fig. 5a). The thermal demagnetization of the IRM showed that (1) in some samples there is an intensity drop before the 200 °C step due to a soft magnetic component (e.g. goethite), (2) a second intensity drop between 400 and 500 °C is probably due to the removal of maghemite, (3) the majority of the samples have a remanence unblocked around 550–600 °C indicating that magnetite is the main magnetic carrier. (4) Finally, about 25% of the samples are not totally demagnetized at 600 °C. If they are not remagnetized because of their progressive heating, some display an intensity drop at 680–700 °C step. This last group of samples probably contains portions of hematite as the prevailing magnetic carrier (Fig. 5b). The dominance of magnetite and the presence of goethite (in some cases) are also confirmed by the thermomagnetic analysis, as shown in Fig. 5c.

The section presents a succession of 12 normal and reverse polarity zones. This polarity succession is characterized by a 42-m thick reverse zone in the middle part; below this, short normal zones alternate with short reverse ones and near the top of the section a normal zone reaches a thickness of 33 m (Fig. 6).

### 4.2. Lavas

At least one specimen per core has been stepwise demagnetized either by AF or thermally. However, AF treatment yielded more consistent results overall. The mean destructive field was in the order of 70 mT, with an unblocking temperature around 580 °C. The low field magnetic susceptibility for pilot samples was measured after each heating step. No significant change is shown up to 400 °C but after this step a regular and progressive

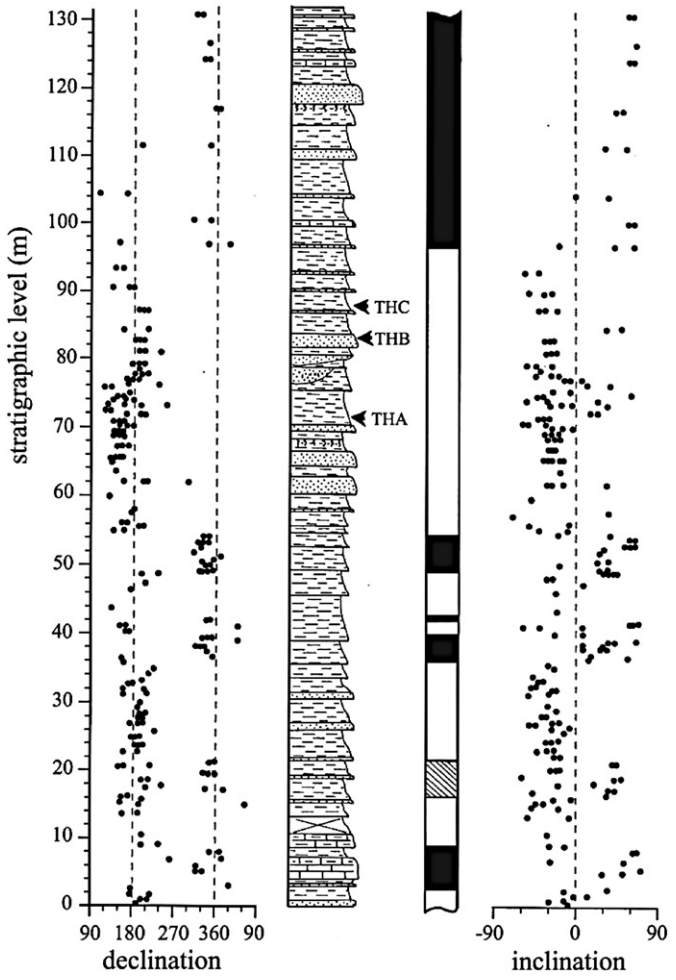


**Fig. 6.** Declination and inclination of the primary magnetization of the sedimentary section and the composed magnetostratigraphic section.

decrease is seen in almost all samples. This change can explain the unsatisfactory response of the samples to the thermal cleaning. Typical demagnetization diagrams are shown in Fig. 7. In most cases the primary component could be calculated by using the best fit towards the origin. Nevertheless some samples submitted to thermal treatment show totally aberrant demagnetization curves and have been rejected from the calculation of the mean direction. The obtained main directions in lavas are of normal polarity in the Emporios complex, mixed polarities in Komi and reverse polarity in the other sites (Table 1). IRM and thermomagnetic results are consistent with magnetite as the main magnetic carrier (Fig. 8).

## 5. Discussion

### 5.1. Statistical treatment

The 93 reliable ChRM directions obtained from the Michalos section, following the above described analysis, are shown in the stereographic projection of Fig. 9. The Vandamme (1994) variable cut-off procedure was applied to discard four widely outlying directions. Thus, only four directions were eliminated. Application of a fixed 45° cut-off, such as advocated by Johnson et al. (2008) gave very similar results. The average direction and cones of confidence were determined using Fisher (1953) statistics applied on virtual geomagnetic poles (VGP), because these are more Fisherian (i.e. a Gaussian dispersion on a sphere) than directions, which have a (latitude dependent) elongated distribution (Tauxe and Kent, 2004; Tauxe et al., 2008; Deenen et al., submitted for publication). Errors in declination and inclination are given separately, as $\Delta$Dx and $\Delta$Ix, following Butler (1992) and Deenen et al. (submitted for publication) (Table 1). A calculated mean direction for the sedimentary succession converted to uniform normal polarity, is $D = 348.1^\circ$, $I = 38.5^\circ$, $\Delta Dx = 5.1$, $\Delta Ix = 6.7$, $N = 89$, A95 = 4.7, $K = 11.2$, after the appropriate tectonic corrections.

The expected inclination at the latitude of Chios at the present day is ~58°, i.e. which is much steeper than the results obtained from the Michalos section. A method to correct for sediment compaction-induced flattening of the inclination is the elongation–inclination (E/I) method proposed by Tauxe and Kent (2004) (assuming a strictly dipolar magnetic field). Even though Tauxe and Kent (2004) suggested a minimum of 100 individual directions for a successful application of this method, we have subjected the 89 directions obtained from the Michalos section to this method to test whether flattening-correction would yield a direction more consistent with the prevailing dipole geomagnetic field. Thus, the inclination would be corrected to $61.8 \pm 3.9^\circ$, i.e. in line with the expected inclination at the latitude of Chios (Fig. 10). The flattening factor of 0.39 (Fig. 10) is within the range of typical flattening values (Krijgsman and Tauxe, 2004; Tauxe and Kent, 2004; Dupont-Nivet et al., submitted for publication). We therefore suggest the flattening-corrected direction of $D = 348.1^\circ$, $I = 61.0^\circ$, $\Delta Dx = 6.1$, $\Delta Ix = 3.9$, $N = 89$, A95 = 4.5, $K = 16.5$.

Recently, Deenen et al. (submitted for publication) have defined reliability criteria for palaeomagnetic data to test whether an observed distribution can be straightforwardly explained by palaeosecular variation (PSV) alone. Therefore, they introduced the terms A95min and A95max, which form an envelope around the possible range of A95 values as a function of $n$ (the amount of averaged spot readings) for the vast majority of PSV scatters that have been reconstructed throughout earth history, from equator to pole (McFadden et al., 1991; Biggin et al., 2008a,b; Lawrence et al., 2009): a VGP distribution with an A95 lower than A95min underrepresents PSV (e.g. due to remagnetization, sampling too short a time span, or smoothing of PSV within individual sediment cores), whereas an A95 higher than A95max likely contains an additional source of scatter besides PSV (e.g. rotation differences within the locality, unresolved overprints, large orientation or measurement errors). With $n = 89$, A95min = 3.0 and A95max = 4.5, our obtained value of A95 = 4.5 lies (just) within the confidence envelope and we therefore have no reason to infer significant within-section rotation differences or abnormally high measuring or remagnetization errors.

A reversal test was performed for the sediments, where both normal and reverse polarities are observed. According to the classification of McFadden and McElhinny (1990) the sediments yield a positive test of Class A ($\gamma_c = 4.94$).

Lava sites should represent spot readings of the Earth's magnetic field, and within-site scatter should be randomly dispersed. Accordingly we applied Fisher (1953) statistics to sample component directions from single lavas (Table 1). Because dispersion within a single lava site should be minimal, we discarded all lava sites with a $k$-value lower than 50 (which corresponds to an $\alpha 95$ of ~8–11° for typical $n$ in lava sites (i.e. 5–8)), following e.g. Biggin et al. (2008a), Johnson et al. (2008) and Deenen et al. (submitted for publication). Thus, sites Emp4, and 5 were rejected, as well as site Arg. The resulting 5 sites were averaged, to yield an average direction of $D = 288.4^\circ$, $I = 25.6^\circ$, $\Delta Dx = 19.8$, $\Delta Ix = 33.0$, $N = 5$, A95 = 16.8, $K = 17.4$. Although errors are very large owing to the low number of averaged lavas, A95 is still within the confidence envelope of Deenen et al. (submitted for publication). The result suggests an ill-defined, yet large counterclockwise rotation.

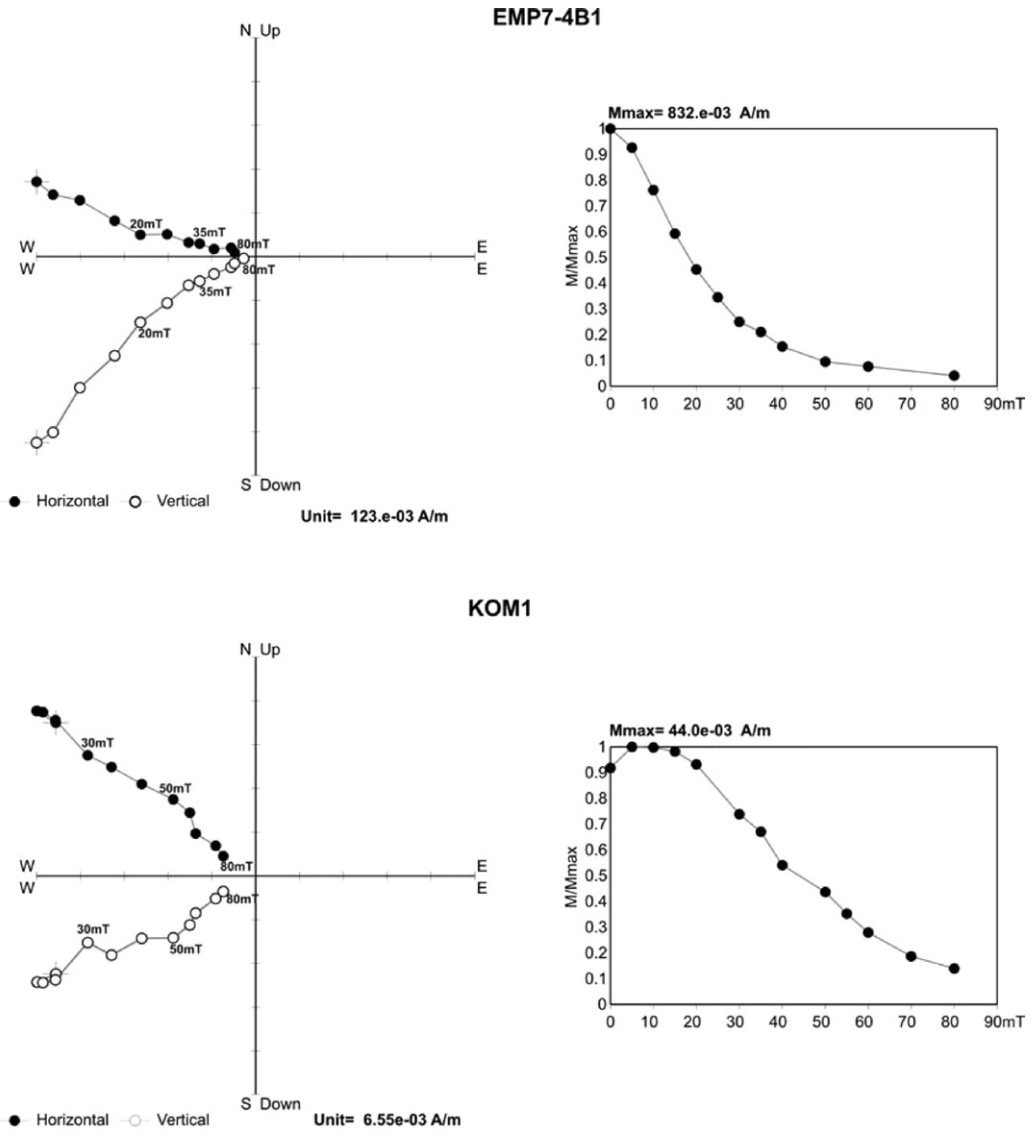


**Fig. 7.** Demagnetization diagrams (Zijderveld diagrams, intensity decay curves) for representative volcanic samples.

**Table 1**
Statistical results for the new data presented here from Chios.

| Locality | Geographical coordinates | $n$ | $D$ | $I$ | $k$ | $\alpha 95$ | Site averages | | | | A95min | A95max |
|---|---|---|---|---|---|---|---|---|---|---|---|---|
| | | | | | | | ΔDx | ΔIx | $K$ | A95 | | |
| Sediments (before TK03) | 38.3°/26.1° | 89 | 348.1 | 38.5 | | | 5.1 | 7 | 11.2 | 4.7 | 3.0 | 4.5 |
| Sediments (after TK03) | | 89 | 348.1 | 61.0 | | | 6.1 | 4 | 16.5 | 4.5 | 3.0 | 4.5 |
| Lavas | | 5 | 288.4 | 25.6 | | | 19.8 | 33 | 17.4 | 16.8 | 7.6 | 31.8 |
| Emp 1–2 | 38.15°/26° | 6 | 278.3 | 36.0 | 59.5 | 8.8 | | | | | | |
| Emp 3 | 38.15°/26° | 4 | 274.8 | 22.6 | 150.9 | 7.5 | | | | | | |
| Emp 4* | 38.19°/26.03° | 3 | 323.3 | 52.5 | 24.8 | 25.3 | | | | | | |
| Emp 5* | 38.19°/26.02° | 3 | 310.5 | 46.7 | 21.8 | 27.1 | | | | | | |
| Emp 6 | 38.19°/26.02° | 3 | 308.5 | 18.8 | 60.8 | 16.0 | | | | | | |
| Emp 7 | 38.15°/26° | 4 | 269.1 | 18.6 | 70.4 | 11.0 | | | | | | |
| Kom | 38.2°/26.05° | 8 | 311.2 | 26.4 | 68.7 | 6.7 | | | | | | |
| Arg* | 38.58°/25.9° | 8 | 309.0 | 40.0 | 10.1 | 25.3 | | | | | | |

$N(n)$ = amount of samples (specimens); $D$ = declination, $I$ = inclination, $k(K)$ = (Fisher, 1953) precision parameter on directions (virtual geomagnetic poles); $\alpha 95$(A95) = 95% cone of confidence of directions (virtual geomagnetic poles); ΔDx = error bar on declination; ΔIx = error bar on inclination (following Butler, 1992); A95min and A95max span the $n$-dependent confidence envelope of (Deenen et al., submitted for publication).

* Site rejected based on too large dispersion ($k$). See text.

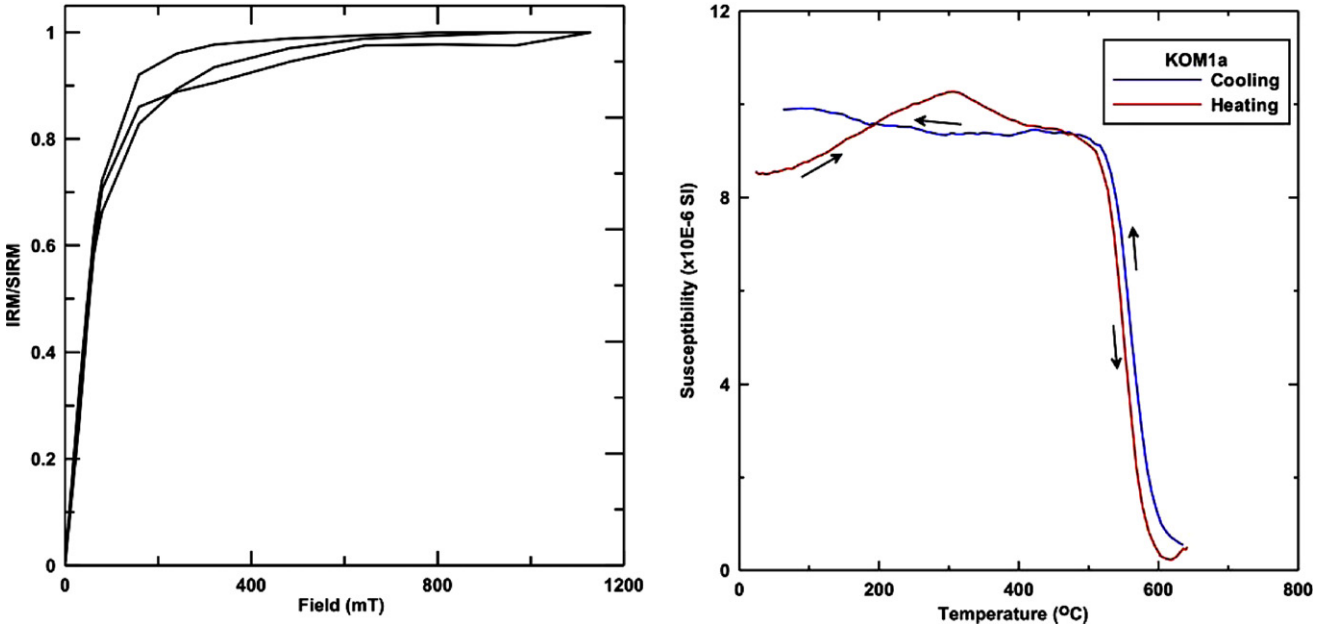


**Fig. 8.** IRM and thermomagnetic curves from selected volcanic samples showing the dominance of magnetite as the main magnetic carrier.

### 5.2. Implications from the obtained palaeomagnetic declinations

Compared to the most recent APWP (Torsvik et al., 2008), the results of the Michalos section on Chios suggest a ~15° counterclockwise vertical axis rotation. In adjacent western Turkey and on the island of Lesbos, no significant regional deviations of the Middle Miocene palaeomagnetic declination from the APWP have been found north of the central Menderes Massif and south of the North Anatolian Fault Zone (Kissel et al., 1989; Beck et al., 2001; van Hinsbergen et al., 2010a). On the contrary, regional counterclockwise rotations occur in south-western Turkey (Kissel and Poisson, 1987; Morris and Robertson, 1993; van Hinsbergen et al., 2010a,b). The rotation of Chios may thus record (part of) the southwest Anatolian rotations, or be affected by local rotations (Fig. 11).

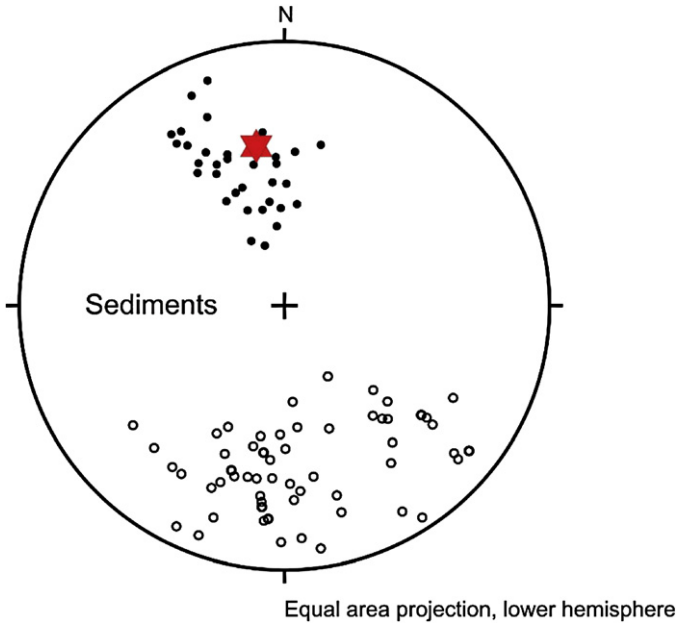


**Fig. 9.** Equal area projections of sediment ChRM directions. The star represents the mean direction from all data.

To distinguish between these, we take the regional structural framework into account. The southwest Anatolian rotating domain has a rotation pole at the eastern limit of the Central Menderes Massif. From there, the amount of N–S extension accommodating the rotation with respect to NW Turkey and Lesbos must increase westward. Large scale extension (of many tens of kilometers) is widespread in the Aegean region and is accommodated by exhumation of metamorphic rocks along extensional detachments (Gautier et al., 1993; Ring et al., 1999a, 2003; Jolivet and Faccenna, 2000; Bozkurt and Oberhänsli, 2001; Jolivet et al., 2003; Jolivet and Brun, 2010). The central Menderes Massif is bounded in the north by the Alaşehir extensional detachment (Hetzel et al., 1995; Işik et al., 2003). This is accommodated, in part, the exhumation of the Central Menderes Massif, and forms the northern limit of the vertical axis rotations in south-western Turkey (van Hinsbergen et al., 2010a). Even though an E–W trending extensional structure may be present between Lesbos and Chios, absence of Cenozoic metamorphic rocks here makes it unlikely that this structure has major displacements. Instead, major back-arc extension in the eastern Aegean region is accommodated along a detachment system south of Chios and the Karaburun peninsula, exhuming metamorphic rocks on the islands of Samos and Ikaria (Ring et al., 1999b; Kumerics et al., 2005). Chios therefore seems structurally not to belong to south-western Anatolian domain which recorded a ~25° rotation with respect to the northwestern part. Furthermore, the absence of significant vertical axis rotations since ~12 Ma on the island of Samos (Sen and Valet, 1986; Kostopoulos et al., 2003) suggests that either regional rotation of southwest Anatolia is accommodated further south, or is limited to the region south of the central Menderes Massif.

Even though the Michalos section provides no reason to assume within-section rotation differences, the few lavas presented in this paper display a poorly defined, but much larger rotation than the Michalos section. This may lend credibility to the inference that the rotations on Chios have local origin. Local rotations along the Greek–Turkish boundary are not uncommon. For example, Lower Miocene (15–18.5 Ma) volcanics of the adjacent Karaburun peninsula yield significant clockwise rotations, as does the region around

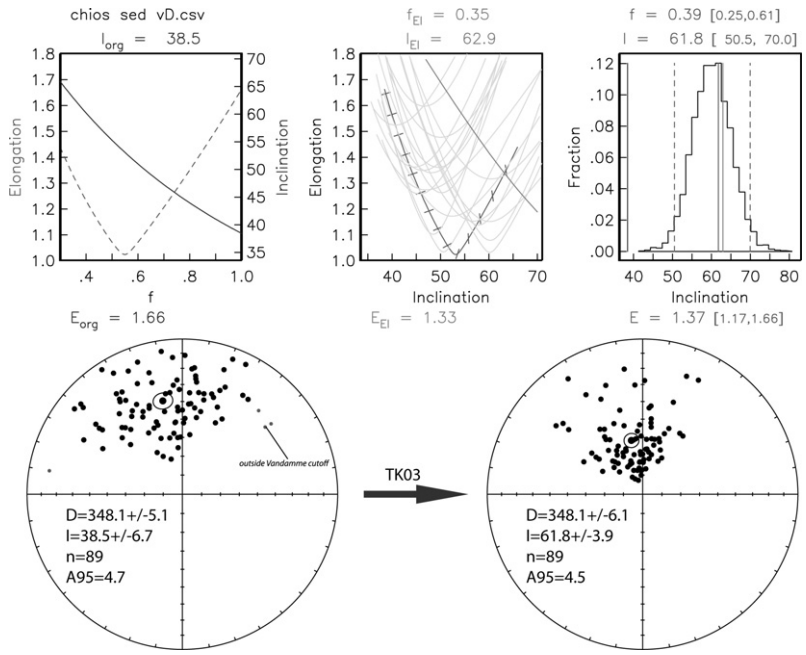


**Fig. 10.** Plots of elongation and inclination versus flattening factor ($f$), as well as elongation versus inclination (red line) for the TK03.GAD model (Tauxe and Kent, 2004), for the data of the Michalos section, for different values of the flattening factor ($f = 0.3 \rightarrow 1.0$). $I_{org}$ = original inclination; $I_{E/I}$ = bootstrapping results for the inclination; $I$ = corrected inclination. The barbs on the red line (B) indicate the direction of elongation of the directional distributions, with horizontal being E–W and vertical being N–S. Also shown are results from 20 bootstrapped data sets (yellow lines, B). The crossing points represent the inclination/elongation pair most consistent with the TK03.GAD model (green line). The histograms represent the crossing points from 5000 bootstrapped data sets and determine the most frequent inclination (vertical red line) with 95% bounds (dashed red lines, C), compared to the original inclination (blue line, C) and the crossing points of the original distribution (green line, C). The corrected inclination (D and E) is in good agreement with the geocentric axial dipole (GAD) inclination (58°) for the present latitude of Chios. (For interpretation of the references to color in this figure caption, the reader is referred to the web version of the article.)

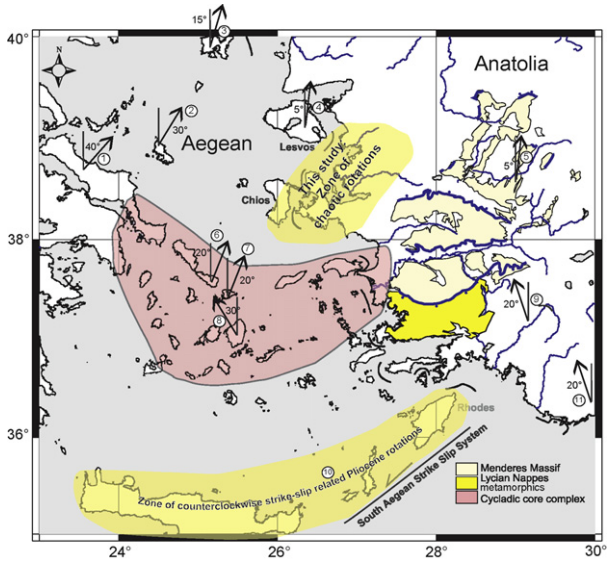


**Fig. 11.** Map of eastern Aegean and western Turkey, showing schematically the main declination distribution from Oligocene and Neogene sediments. *Key to references*: (1) Evvia: Kissel et al. (1986b), Morris (1995), see also Kissel and Laj (1988) and van Hinsbergen et al. (2005a,b, 2008) for the wider west-Aegean region with large clockwise Neogene rotations; (2) Skyros: Kissel et al. (1986b); (3) Lemnos: Westphal and Kondopoulou (1993); (4) Lesvos: Kissel et al. (1989) and Beck et al. (2001); (5) Northern Menderes Massif Miocene volcano-sedimentary basins: van Hinsbergen et al. (2010a); (6) Tinos: Avigad et al. (1998); (7) Mykonos: Morris and Anderson (1996); (8) Naxos: Morris and Anderson (1996); (9) Neogene basins Lycian Nappes: van Hinsbergen et al. (2010a); (10) Southeastern Aegean region (Crete, Karpathos, Rhodos): Duermeijer et al. (1998, 2000) and van Hinsbergen et al. (2007); (11) Bey Dağları: Kissel and Poisson (1987), Morris and Robertson (1993) and van Hinsbergen et al. (2010b).

Foca (Kissel et al., 1987; Kissel and Laj, 1988), whereas the Dikili and Yuntdağ mountains provide a scatter of directions from lava sites that clearly indicate strong within-locality rotations (van Hinsbergen et al., 2010a). Thus, a zone roughly parallel to the coast may be identified as one of chaotic vertical axis rotations. Recently, this zone was postulated to accommodate left-lateral transform motions of Greece with respect to western Turkey, coinciding with the eastern limits of the Anatolide-Tauride basement of the Menderes Massif (Ring et al., 1999a; Özkaymak and Sözbilir, 2008; Uzel and Sözbilir, 2008; Erkül, 2010; van Hinsbergen et al., 2010a). This transform zone could translate extensional exhumation of the Cycladic detachments to the Menderes detachments, which extend much further to the north, and accommodate the difference between larger amounts of extension in Greece than Turkey. The detailed relations between individual faults and their influence on local block rotations is beyond the scope of this study, but the zone affected by local vertical axis rotations, previously identified in western Turkey (van Hinsbergen et al., 2010a,b; Fig. 1) includes the island of Chios.

## 6. Conclusions

We present new palaeomagnetic data from Middle Miocene sediments and lavas from the Island of Chios in the Eastern Aegean region. The quality of the magnetic signature was more satisfying in sediments than in lavas, and provides evidence for a significant 15° counterclockwise rotation. An inclination derived from these sediments of 38° was corrected to 61° using the elongation/inclination method, which is within error of the expected palaeomagnetic inclination at the latitude of Chios.

Rotation results for a small set of five lavas provide a poorly defined, but significantly larger rotation of approximately 70° counterclockwise. Albeit poorly defined, these results indicate

that the rotation pattern is not consistent on the scale of Chios Island.

The regional palaeomagnetic pattern of the Aegean and west Anatolian regions displays evidence for an orocline that formed since Middle Miocene times. Oroclinal bending appears to have concentrated in the external parts of the Aegean back-arc, and was at least partly accommodated by back-arc extension. Chios is located to the north of the main extensional province of Greece – the Cycladic metamorphic core complex – and to the west of the Menderes metamorphic core complexes of western Turkey. As such, it likely belongs to the non-rotating, relatively stable northern portion of the Aegean orocline. The rotations of Chios are hence most likely part of a zone of chaotic rotations that includes the west Anatolian Karaburun peninsula and the Dikili, Foca and Yuntdağ volcanic regions. This zone may form a band of transform motions that link the northern Menderes Massif with the Cyclades, and that accommodates a westward increase in back-arc extensional strain from western Turkey to Greece.

## Acknowledgements

This work was carried out over a period of several years and was funded by: the Greek National Research Foundation, the Geophysical Laboratory of Aristotle University and the French CNRS. Palaeomagnetic laboratories of IPGP and École Normale Supérieure (Paris) are acknowledged for providing equipment access. Palaeomagnetic data were partly analyzed using Gmagtools provided by R. Enkin. Drs. Ph. Voidomatis, K. Kolliadimou, and G. Syrides helped with sampling. E. Bozkurt and two anonymous reviewers are warmly thanked for providing extensive and constructive comments on the original version of the manuscript. Finally Prof. Emeritus B. Papazachos is thanked for a grant which allowed the final field trip to take place. DJJvH acknowledges Statoil for financial support (SPlates Model project).

## References

Aidona, E., Kondopoulou, D.P., Scholger, R., Georgakopoulos, A., Vafeidis, A., 2008. Palaeomagnetic investigations of sediments cores from Axios zone (N. Greece): implications of low inclinations in the Aegean. eEarth 3, 7–18.

Atzemoglou, A., Kondopoulou, D., Papamarinopoulos, S., Dimitriadis, S., 1994. Palaeomagnetic evidence for block rotations in the Western Greek Rhodope. Geophysical Journal International 118 (1), 221–230.

Avigad, D., Baer, G., Heimann, A., 1998. Block rotations and continental extension in the central Aegean Sea: palaeomagnetic and structural evidence from Tinos and Mykonos, Cyclades, Greece. Earth and Planetary Science Letters 157, 23–40.

Beck, M.E., Burmester, R.F., Kondopoulou, D.P., Atzemoglou, A., 2001. The palaeomagnetism of Lesbos, NE Aegean, and the eastern Mediterranean inclination anomaly. Geophysical Journal International 145, 233–245.

Bellon, H., Jarrige, J.J., Sorel, D., 1979. Les activités magmatiques égéennes de l'Oligocène à nos jurs et leurs cadres géodynamiques. Données nouvelles et synthèse. Revue de Geologie Dynamique et de Geographie Physique 21, 41–55.

Besenecker, H., 1973. Neogen und Quartär der Insel Chios (Ägäis) (Thesis), Freien Univertsität Berlin, Berlin, 196 pp.

Besenecker, H., Pichler, H., 1974. Die junen Vulkanite der Insel Chios (ostliche Agais, Griechenland). Geologisches Jahrbuch D9, 41–65.

Biggin, A., van Hinsbergen, D.J.J., Langereis, C.G., Straathof, G.B., Deenen, M.H., 2008a. Geomagnetic secular variation in the Cretaceous normal superchron and in the Jurassic. Physics of the Earth and Planetary Interiors 169, 3–19.

Biggin, A.J., Strik, G.H.M.A., Langereis, C.G., 2008b. Evidence for a very-long-term trend in geomagnetic secular variation. Nature Geoscience 1, 395–398.

Bozkurt, E., Oberhänsli, R., 2001. Menderes Massif (Western Turkey): structural, metamorphic and magmatic evolution—a synthesis. International Journal of Earth Sciences 89, 679–708.

Brun, J.-P., Sokoutis, D., 2007. Kinematics of the Southern Rhodope core complex (Northern Greece). International Journal of Earth Sciences 96, 1079–1099.

Butler, R.F., 1992. Palaeomagnetism: Magnetic Domains to Geologic Terranes. Blackwell Scientific Publications, Boston, 195 pp.

Deenen, M.H.L., Langereis, C.G., van Hinsbergen, D.J.J., Biggin, A.J., submitted for publication, Geomagnetic secular variation and the statistics of palaeomagnetic directions. Geophysical Journal International.

Duermeijer, C.E., Krijgsman, W., Langereis, C.G., ten Veen, J.H., 1998. Post early Messinian counter-clockwise rotations on Crete: implications for the late Miocene to recent kinematics of the southern Hellenic Arc. Tectonophysics 298 (1–3), 77–89.

Duermeijer, C.E., Nyst, M., Meijer, P.T., Langereis, C.G., Spakman, W., 2000. Neogene evolution of the Aegean arc: palaeomagnetic and geodetic evidence for a rapid and young rotation phase. Earth and Planetary Science Letters 176, 509–525.

Dunlop, D., Özdemir, Ö., 1997. Rock: Magnetism Fundamentals and Frontiers. Cambridge University Press, Cambridge, 573 pp.

Dupont-Nivet, G., van Hinsbergen, D.J.J., Torsvik, T.H., submitted for publication. Persistently low Asian palaeolatitudes: implications for the Indo-Asia collision. Tectonics.

Erkül, F., 2010. Tectonic significance of synextensional ductile shear zones within the early Miocene Alacamdag granites, northwestern Turkey. Geological Magazine, doi:10.1017/S0016756809990719.

Fisher, R.A., 1953. Dispersion on a sphere. Proceedings of the Royal Society of London A217, 295–305.

Forster, M.A., Lister, G.S., 2009. Core-complex-related extension of the Aegean lithosphere initiated at the Eocene–Oligocene transition. Journal of Geophysical Research 114, B02401, doi:10.1029/2007JB005382.

Gautier, P., Brun, J.-P., Jolivet, L., 1993. Structure and kinematics of upper Cenozoic extensional detachment on Naxos and Paros. Tectonics 12 (5), 1180–1194.

Gautier, P., Brun, J.-P., 1994. Crustal-scale geometry and kinematics of late-orogenic extension in the central Aegean (Cyclades and Evvia island). Tectonophysics 238, 399–424.

Govers, R., Wortel, M.J.R., 2005. Lithosphere tearing at STEP faults: response to edges of subduction zones. Earth and Planetary Science Letters 236, 505–523.

Hetzel, R., Ring, U., Akal, C., Troesch, M., 1995. Miocene NNE-directed extensional unroofing in the Menderes Massif, southwestern Turkey. Journal of the Geological Society of London 152, 639–654.

Işik, V, Tekeli, O., 2001. Late orogenic crustal extension in the northern Menderes massif (western Turkey): evidence for metamorphic core complex formation. International Journal of Earth Sciences 89, 757–765.

Işik, V., Seyitoğlu, G., Çemen, I., 2003. Ductile-brittle transition along the Alasehir detachment fault and its structural relationship with the Simav detachment fault, Menderes massif, western Turkey. Tectonophysics 374, 1–18.

Işik, V., Tekeli, O., Seyitoğlu, G., 2004. The 40Ar/39Ar age of extensional ductile deformation and granitoid intrusion in the northern Menderes core complex: implications for the initiation of extensional tectonics in western Turkey. Journal of Asian Earth Sciences 23, 555–566.

Jacobshagen, V., 1986. Geologie von Griechenland. Borntraeger, Berlin, Stuttgart, 279 pp.

Johnson, C.L., Constable, C.G., Tauxe, L., Barendregt, R., Brown, L.L., Coe, R.S., Layer, P., Mejia, V., Opdyke, N.D., Singer, B.S., Staudigel, H., Stone, D.B., 2008. Recent investigations of the 0–5 Ma geomagnetic field recorded by lava flows. Geochemistry, Geophysics, Geosystems 9, Q04032, doi:10.1029.2007GC001696.

Jolivet, L., Brun, J.-P., Gautier, P., Lallemant, S., Patriat, M., 1994. 3D-kinematics of extension in the Aegean region from the early Miocene to the present, insights from the ductile crust. Bulletin de la Societe Geologique de France 165 (3), 195–209.

Jolivet, L., Faccenna, C., 2000. Mediterranean extension and the Africa–Eurasia collision. Tectonics 19 (6), 1094–1106.

Jolivet, L., 2001. A comparison of geodetic and finite strain pattern in the Aegean, geodynamic implications. Earth and Planetary Science Letters 187, 95–104.

Jolivet, L., Facenna, C., Goffé, B., Burov, E., Agard, P., 2003. Subduction tectonics and exhumation of high-pressure metamorphic rocks in the Mediterranean orogen. American Journal of Science 303, 353–409.

Jolivet, L., Brun, J.-P., 2010. Cenozoic geodynamic evolution of the Aegean. International Journal of Earth Sciences 99, 109–138.

Jolivet, L., Lecomte, E., Huet, B., Denèle, Y., Lacombe, O., Labrousse, L., Le Pourhiet, L., Mehl, C., 2010. The North Cycladic detachment system. Earth and Planetary Science Letters 289, 87–104.

Karakostas, V., Papadimitriou, E.E., Tranos, M.D., Papazachos, C.B., 2010. Active seismotectonic structures in the area of Chios Island, North Aegean Sea, revealed from microseismicity and fault plane solutions. Bulletin of the Geological Society of Greece XLIII (4), 2053–2064.

Kaymakci, N., Aldanmaz, E., Langereis, C.G., Spell, T.L., Gurer, O.F., Zanetti, K.A., 2007. Late Miocene transcurrent tectonics in NW Turkey: evidence from palaeomagnetism and 40Ar-39Ar dating of alkaline volcanic rocks. Geological Magazine 144, 379–392.

Kilias, A.A., 1982. Kleintektonische Untersuchungen im nordlich Teil der Insel Chios. Annals, Faculty of Physics and Mathematics, University of Thessaloniki 22, 3–20.

Kirschvink, J.L., 1980. The least-squares line and plane and the analysis of palaeomagnetic data. Geophysical Journal of the Royal Astrological Society 62, 699–718.

Kissel, C., Laj, C., Poisson, A., Savascin, Y., Simeakis, K., Mercier, J.L., 1986a. Palaeomagnetic evidence for Neogene rotational deformations in the Aegean domain. Tectonics 5, 783–796.

Kissel, C., Laj, C., Mazaud, A., 1986b. First palaeomagnetic results from Neogene formations in Evia, Skyros and the Volos region and the deformation of Central Aegea. Geophysical Research Letters 13, 1446–1449.

Kissel, C., Laj, C., Şengör, A.M.C., Poisson, A., 1987. Palaeomagnetic evidence for rotation in opposite senses of adjacent blocks in northeastern Aegean and western Anatolia. Geophysical Research Letters 14 (9), 907–910.

Kissel, C., Poisson, A., 1987. Étude paléomagnetique préliminaire des formations cénozoïques de Bey Daglari (Taurides occidentales, Turquie). Comptes Rendus des Academie Sciences Paris 304 (Série II (8)), 343–348.

Kissel, C., Laj, C., 1988. The tertiary geodynamical evolution of the Aegean arc: a palaeomagnetic reconstruction. Tectonophysics 146, 183–201.

Kissel, C., Laj, C., Poisson, A., Simeakis, K., 1989. A pattern of block rotations in central Aegean. In: Kissel, C., Laj, C. (Eds.), Palaeomagnetic Rotations and Continental Deformation. Kluwer Academic Publishers, pp. 115–129.

Kondopoulou, D.P., Lauer, J.P., 1984. Palaeomagnetic data from Tertiary units of the North Aegean zone. In: Dixon, J.E., Robertson, A.H.F. (Eds.), The Geological Evolution of the Eastern Mediterranean. Geological Society of London Special Publications, pp. 681–686.

Kondopoulou, D., De Bonis, L., Koufos, G., Sen, S., 1993a. Palaeomagnetic data and biostratigraphy of the Middle Miocene vertebrate locality of Thymiana, Chios island, Greece. In: Proceedings of the 2nd Congress of the Hellenic Geophysical Union, Florina, pp. 676–687.

Kondopoulou, D., Leci, V., Symeakis, C., 1993b. Palaeomagnetic study of the Tertiary volcanics in Chios Island, Greece. In: Proceedings of the 2nd Congress of the Hellenic Geophysical Union, Florina, pp. 676–687.

Kondopoulou, D., 2000. Palaeomagnetism in Greece: Cenozoic and Mesozoic components and their geodynamic implications. Tectonophysics 326, 131–151.

Kondopoulou, D., Zananiri, I., Michard, A., Feinberg, H., Atzemoglou, A., Pozzi, J.-P., Voidomatis, Ph., 2007. Neogene tectonic rotations in the vicinity of the North Aegean trough: new palaeomagnetic evidence from Athos and Samothraki (Greece). Bulletin of the Geological Society of Greece XXXVII, 343–359.

Kostopoulos, D.S., Sen, S., Koufos, G.D., 2003. Magnetostratigraphy and revised chronology of the late Miocene mammal localities of Samos, Greece. International Journal of Earth Sciences 92, 779–794.

Koufos, G.D., de Bonis, L., Sen, S., 1995. Lophocyon paraskevaidisi, a new viverrid (Carnivora, Mammalia) from the Middle Miocene of Chios island, Greece. Geobios 28, 511–523.

Krijgsman, W., Tauxe, L., 2004. Shallow bias in the Mediterranean palaeomagnetic directions caused by inclination error. Earth and Planetary Science Letters 222 (2), 685–695.

Kumerics, C., Ring, U., Bricheau, S., Glodny, J., Monié, P., 2005. The extensional Messaria shear zone and associated brittle detachment faults, Aegean Sea, Greece. Journal of the Geological Society of London 162 (4), 701–721.

Lawrence, K.P., Tauxe, L., Staudigel, H., Constable, C.G., Koppers, A.A.P., McIntosh, W., Johnson, C.L., 2009. Palaeomagnetic field properties at high southern latitude. Geochemistry, Geophysics, Geosystems 10, Q01005, doi:10.1029/2008GC002072.

McFadden, P.C., McElhinny, M.W., 1990. Classification of the reversal test in palaeomagnetism. Geophysical Journal International 103, 725–729.

McFadden, P.L., Merril, R.T., McElhinny, M.W., Lee, S., 1991. Reversals of the Earth's magnetic field and temporal variations of the dynamo families. Journal of Geophysical Research 96, 3923–3933.

Morris, A., 1995. Rotational deformation during Palaeogene thrusting and basin closure in eastern central Greece: palaeomagnetic evidence from Mesozoic carbonates. Geophysical Journal International 121, 827–847.

Morris, A., Anderson, M., 1996. First palaeomagnetic results from the Cycladic Massif, Greece, and their implications for Miocene extension directions and tectonic models in the Aegean. Earth and Planetary Science Letters 142, 397–408.

Morris, A., Robertson, A.H.F., 1993. Miocene remagnetisation of carbonate platform and Antalya Complex units within the Isparta angle, SW Turkey. Tectonophysics 220, 243–266.

Ocakoğlu, N., Demirbağ, E., Kuşçu, I., 2005. Neotectonic structures in Izmir Gulf and surrounding regions (western Turkey): evidences of strike-slip faulting with compression in the Aegean extensional regime. Marine Geology 219, 155–171.

Orbay, N., Sanver, M., Hisarli, T., Isseven, T., Ozcep, F., 2000. Karaburun Yarimadasinin paleomagnetizmasi ve tektonik evrimi. Bati Anadolu' nun Depremselliği Sempozyumu kitabi, 59–67.

Özkaymak, Ç., Sözbilir, H., 2008. Stratigraphic and structural evidence for fault reactivation: the active Manisa fault zone, Western Anatolia. Turkish Journal of Earth Sciences 17, 615–635.

Paraskevaidis, I., 1940. Eine obermiocane fauna von Chios. Neues Jahrbuch fvr Mineralogie Geologie und Paläontologie 83, 363–442.

Pe-Piper, G., Piper, D.J.W., 1989. Spatial and temporal variation in Late Cenozoic back-arc volcanic rocks, Aegean Sea region. Tectonophysics 169, 113–134.

Piper, J.D.A., Gursoy, H., Tatar, O., Beck, M.E., Rao, A., Koçbulut, F., Mesci, B.L., 2009. Distributed neotectonic deformation in the Anatolides of Turkey: a palaeomagnetic analysis. Tectonophysics, doi:10.1016/j.tecto.2009.05.026.

Ricou, L.-E., Burg, J.-P., Godfriaux, I., Ivanov, Z., 1998. Rhodope and Vardar: the metamorphic and the olistostromic paired belts related to the Cretaceous subduction under Europe. Geodynamica Acta 11 (6), 285–309.

Ring, U., Gessner, K., Güngör, T., Passchier, C.W., 1999a. The Menderes Massif of western Turkey and the Cycladic Massif in the Aegean—do they really correlate? Journal of the Geological Society of London 156, 3–6.

Ring, U., Laws, S., Bernet, M., 1999b. Structural analysis of a complex nappe sequence and late-orogenic basins from the Aegean Island of Samos. Journal of Structural Geology 21, 1575–1601.

Ring, U., Layer, P.W., Reischmann, T., 2001. Miocene high-pressure metamorphism in the Cyclades and Crete, Aegean Sea, Greece: evidence for large-magnitude displacement on the Cretan detachment. Geology 29 (5), 395–398.

Ring, U., Johnson, C., Hetzel, R., Gessner, K., 2003. Tectonic denudation of a Late Cretaceous-Tertiary collisional belt: regionally symmetric cooling patterns and their relation to extensional faults in the Anatolide belt of western Turkey. Geological Magazine 140 (4), 421–441.

Ring, U., Glodny, J., Will, T., Thomson, S.N., 2010. The Hellenic subduction system: high-pressure metamorphism, exhumation, normal faulting, and large-scale extension. Annual Review of Earth and Planetary Sciences 38, 45–76.

Rothausen, K., 1977. Die mittelmiozanen Wirbertierfund-stellen sudlich Thymiana (Insel Chios, Agais, Griechenland). Teil: Geologie: Die Fundstellen und ihre Abfolge. Annulaire Geologique de Pays Hellenique 28, 495–515.

Schmid, S.M., Berza, T., Diaconescu, V., Froitzheim, N., Fügenschuh, B., 1998. Orogen-parallel extension in the Southern Carpathians. Tectonophysics 297, 209–228.

Sen, S., Valet, J.-P., 1986. Magnetostratigraphy of late Miocene continental deposits in Samos, Greece. Earth and Planetary Science Letters 80, 167–174.

Sen, S., Aidona, E., Kondopoulou, D.P., Koufos, G.D., 2006. Magnetostratigraphy and palaeomagnetism of the Miocene formations of Chios Island, Greece. Travaux Geophysiques XXVII, 101 (Abstract book of the 10th Castle Meeting on Paleo, Rock and Environmental Magnetism, Castle of Valtice, Czech Republic).

Şengör, A.M.C., Yilmaz, Y., 1981. Tethyan evolution of Turkey: a plate tectonic approach. Tectonophysics 75, 181–241.

Tauxe, L., Kent, D.V., 2004. A simplified statistical model for the geomagnetic field and the detection of shallow bias in palaeomagnetic inclinations: was the ancient magnetic field dipolar? In: Channell, J.E.T., Kent, D.V., Lowrie, W., Meert, J.G. (Eds.), Timescales of the Palaeomagnetic Field, Geophysical Monograph. American Geophysical Union, pp. 101–115.

Tauxe, L., Kodama, K.P., Kent, D.V., 2008. Testing corrections for palaeomagnetic inclination error in sedimentary rocks: a comparative approach. Physics of the Earth and Planetary Interiors 169, 152–165.

Tobien, H., 1977. Die Mittelmiozanen Wirbeltierfundstellen sudlich Thymiana (Insel Chios, Agais, Griechenland). Annulaire Geologique de Pays Hellenique 28, 489–494.

Torsvik, T.H., Müller, R.D., Van der Voo, R., Steinberger, B., Gaina, C., 2008. Global plate motion frames: toward a unified model. Reviews of Geophysics 41, RG3004, doi:10.1029/2007RG000227.

Uzel, B., Sözbilir, H., 2008. A first record of a strike-slip basin in western Anatolia and its tectonic implication: the Cumaovası Basin. Turkish Journal of Earth Sciences 17, 559–591.

Uzel, B., Sözbilir, H., Özkaymak, Ç., 2010, Neotectonic evolution of an actively growing superimposed basin in western Anatolia: the inner Bay of İzmir, Turkey. Turkish Journal of Earth Sciences, doi:10.3906/yer-0910-11.

van Hinsbergen, D.J.J., Hafkenscheid, E., Spakman, W., Meulenkamp, J.E., Wortel, M.J.R., 2005a. Nappe stacking resulting from subduction of oceanic and continental lithosphere below Greece. Geology 33 (4), 325–328.

van Hinsbergen, D.J.J., Langereis, C.G., Meulenkamp, J.E., 2005b. Revision of the timing, magnitude and distribution of Neogene rotations in the western Aegean region. Tectonophysics 396, 1–34.

van Hinsbergen, D.J.J., Krijgsman, W., Langereis, C.G., Cornée, J.J., Duermeijer, C.E., van Vugt, N., 2007. Discrete Plio-Pleistocene phases of tilting and counterclockwise rotation in the southeastern Aegean arc (Rhodos, Greece): early Pliocene formation of the south Aegean left-lateral strike-slip system. Journal of the Geological Society of London 164, 1133–1144.

van Hinsbergen, D.J.J., Dupont-Nivet, G., Nakov, R., Oud, K., Panaiotu, C., 2008. No significant post-Eocene rotation of the Moesian Platform and Rhodope (Bulgaria): implications for the kinematic evolution of the Carpathian and Aegean arcs. Earth and Planetary Science Letters 273, 345–358.

van Hinsbergen, D.J.J., Dekkers, M.J., Bozkurt, E., Koopman, M., 2010a. Exhumation with a twist: palaeomagnetic constraints on the evolution of the Menderes metamorphic core complex (western Turkey). Tectonics 29, TC2596, doi:10.1029/2009TC002596.

van Hinsbergen, D.J.J., Dekkers, M.J., Koç, A., 2010b. Testing Miocene remagnetization of Bey Daglari: timing and amount of Neogene rotations in SW Turkey. Turkish Journal of Earth Sciences 19, doi:10.3906/yer-0904-1.

Vandamme, D., 1994. A new method to determine palaeosecular variation. Physics of the Earth and Planetary Interiors 85, 131–142.

Westphal, M., Kondopoulou, D., Edel, J.B., Pavlides, S., 1991. Palaeomagnetism of late Tertiary and Plio-Pleistocene formations form N, Greece. Bulletin of the Geological Society of Greece 25, 239–250.

Westphal, M., Kondopoulou, D., 1993. Palaeomagnetism of Miocene volcanics from Lemnos island: implications for block rotations in the vicinity of the north Aegean Trough. Annales Tectonicae 7 (2), 142–149.

Zananiri, I., Dimitriadis, S., Kondopoulou, D., Atzemoglou, A., 2002. A preliminary AMS study in some Tertiary granitoids from Northern Greece: integration of tectonic and palaeomagnetic data. Physics and Chemistry of the Earth 27, 1289–1297.